5726 J. Phys. Chem. 1985, 89, 5726-5732

Gas Evolution Oscillators. 7. A Quantitative Modeling Test for the Morgan Reaction[1]

Zhi Yuan, Peter Ruoff,† and Richard M. Noyes*

Department of Chemistry, University of Oregon, Eugene, Oregon 97403 *(Received: June 10, 1985)*

A program has been developed to model the pulsed evolution of carbon monoxide produced by the dehydration of formic acid in concentrated sulfuric acid. The program has been tested against experimental measurements reported in the previous paper. The computations used independently measured values of all parameters except k_{ex}, the rate constant for the escape of molecules through the surface of the stirred solution. The value of this quantity was assigned as a disposable parameter for each rate of chemical reaction. Experimentally measured periods, amplitudes, and shapes of pressure vs. time curves were reproduced reasonably well. These assigned values of k_{ex} were larger than those measured for stirred sulfuric acid in which no chemical reaction was taking place. The difference can be rationalized by noting that gas evolution due to chemical reaction is accompanied by considerable foaming which increases the effective surface area of the solution. For any value of k_{ex}, the computations indicate that, regardless of rate of reaction, behavior is an almost unique function of Φ_{xs}, the excess rate of reaction beyond that necessary to bring the steady-state concentration of product gas up to that critical for homogeneous nucleation. Once an oscillating solution attains that critical concentration, times until subsequent maxima and minima in pressure and in concentration are almost independent of rate of chemical reaction. This near independence suggests that differential difference equations might offer a rather simple but effective way to model such systems. Procedures are suggested by which the computations could be further improved, but it is doubtful the effort would be justified by additional insights.

I. Introduction

Morgan[2] discovered that during dehydration of moderately concentrated formic acid in concentrated sulfuric acid, the product carbon monoxide could be emitted in periodic bursts. Experimental measurements by Smith, Noyes, and Bowers[3] indicated that the phenomenon occurred because the solution of dissolved gas became grossly supersaturated before homogeneous nucleation was initiated almost discontinuously. These nuclei grew slowly at first but eventually depleted the dissolved gas faster than it was being produced by chemical reaction. Further nucleation was then inhibited until the bubbles from the first pulse had escaped.

Preliminary computations by Smith[4] supported the validity of the interpretation but had to use unverified estimates of some of the essential parameters. A further analysis of the stability of the steady state[5] suggested that these then unknown parameters could be measured directly, and the model computations could thus be tested by direct comparison with experiment.

Kaushik and Noyes[6] measured or estimated parameters associated with homogeneous nucleation and with transport of molecules and bubbles from solution to gas phase. Kaushik, Rich, and Noyes[7] then evaluated the parameters associated with chemical reaction. They also characterized a specific experimental system for comparison with the results of model computations. In the present paper, those computations are described and compared with experimental observations.

II. Symbols and Units

The various symbols used to describe the system are defined as follows. Dimensions in cgs or other units used in the computations are included for easy reference:

A	area of surface of solution, cm^2
C_{bulk}	concentration of dissolved gas in solution, mol cm^{-3}
C_{crit}	critical concentration for nucleation of bubbles, mol cm^{-3}
C_{sat}	concentration in a solution in equilibrium with gas at pressure P_{gas}, mol cm^{-3}
C^0_{sat}	concentration in equilibrium with gas at pressure P_{atm}, mol cm^{-3}
F	parameter defined in eq IV-4, torr mol^{-1}
g	acceleration of gravity, cm s^{-2}
$j = 1, 2, ..., M$	index number for radius increment
J	rate of formation of nuclei of radius r_1, cm^{-3} s^{-1}
k_{cap}	rate constant for escape of gas through capillary, s^{-1}
k_{ex}	rate constant for transport of molecules from surface of stirred solution to gas, cm s^{-1}
k_{ex}(crit)	value of k_{ex} (for a specific value of Φ_{reac}) at which in the nonoscillatory steady-state $C_{bulk} = C_{crit}$, cm s^{-1}
k_j	rate constant for escape of bubble of radius r_j, s^{-1}
k_{tr}	rate constant for transport of molecules between bubble and solution, cm s^{-1}
M	number of radius increments
N_j	concentration of bubbles having radii in increment j, cm^{-3}
P_{atm}	atmospheric pressure, torr
P_{gas}	pressure of gas in contact with solution in flask, torr
ΔP	excess pressure in flask relative to atmosphere, torr
P_r	pressure of gas in bubble of radius r, torr
q_j	rate constant for conversion of bubble in increment j to increment $j - 1$ or $j + 1$, s^{-1}
r	radius of bubble, cm
r_{eq}	radius of bubble in equilibrium with C_{bulk}, cm
r_j	radius used in computation for any bubble belonging in increment j, cm
r_1	radius of nuclear bubble in equilibrium with C_{crit}, cm
R	gas constant, torr cm^3 mol^{-1} K^{-1}
T	temperature, K
v_{esc}	total rate of escape of gas from solution either as molecules or in bubbles, mol s^{-1}
V_g	volume of gas in flask, cm^3
V_s	volume of solution, cm^3
$\bar{z}$	average distance below surface of a point in the solution, cm
α	parameter in nucleation rate defined in eq IV-9, cm^{-3} s^{-1}
β	parameter in nucleation rate defined in eq IV-9, mol^2 cm^{-6}
Δ_j	width of radius increment j, cm
μ	parameter defined in eq VII-1 indicating asymmetry in oscillations of ΔP

---

† Permanent address: Department of Chemistry, Rogaland Regional College, Ullandhaug, 4001 Stavanger, Norway.

(1) No. 67 in the series "Chemical Oscillations and Instabilities". No. 66 is the preceding paper in this issue.

(2) Morgan, J. S. *J. Chem. Soc., Trans.* **1916**, *109*, 274-283.

(3) Smith, K. W.; Noyes, R. M.; Bowers, P. G. *J. Phys. Chem.* **1983**, *87*, 1514-1519.

(4) Smith, K. W.; Noyes, R. M. *J. Phys. Chem.* **1983**, *87*, 1520-1524.

(5) Noyes, R. M. *J. Phys. Chem.* **1984**, *88*, 2827-2833.

(6) Kaushik, S. M.; Noyes, R. M. *J. Phys. Chem.* **1985**, *89*, 2027-2031.

(7) Kaushik, S. M.; Rich, R. L.; Noyes, R. M. *J. Phys. Chem.* preceding paper in this issue.

0022-3654/85/2089-5726$01.50/0

η	viscosity of solution, g cm^{-1} s^{-1}
κ	Henry's law constant, mol cm^{-3} torr^{-1}
ρ	density of solution, g cm^{-3}
σ	surface tension, cm torr
τ	period of oscillations, s
Φ_{reac}	rate of chemical reaction producing molecules of dissolved gas, mol cm^{-3} s^{-1}
Φ_{crit}	value of Φ_{reac} (for a specific value of k_{ex}) at which in the nonoscillatory steady-state $C_{\text{bulk}} = C_{\text{crit}}$, mol cm^{-3} s^{-1}
Φ_{xs}	excess of rate of production of dissolved gas over the rate at which gas molecules would evaporate from the surface of the solution in a steady state when $C_{\text{bulk}} = C_{\text{crit}}$, mol cm^{-3} s^{-1}

Subscripts max, min, and ss refer respectively to maximum, minimum, and steady-state values of ΔP and C_{bulk}.

III. Relations among Parameters

Equations III-1 to III-12 define several important relationships among the various parameters:

$$\Delta P = P_{\text{gas}} - P_{\text{atm}} \tag{III-1}$$

$$C_{\text{sat}} = \kappa P_{\text{gas}} \tag{III-2}$$

$$C^0_{\text{sat}} = \kappa P_{\text{atm}} \tag{III-3}$$

$$P_r = P_{\text{gas}} + 2\sigma/r \tag{III-4}$$

$$r_{\text{eq}} = \frac{2\kappa\sigma}{C_{\text{bulk}} - C_{\text{sat}}} \tag{III-5}$$

$$r_1 = \frac{2\kappa\sigma}{C_{\text{crit}} - C^0_{\text{sat}}} \tag{III-6}$$

$$r_j = r_1(r_M/r_1)^{(j-1)/(M-1)} \qquad j = 1, 2, ..., M \tag{III-7}$$

$$\Delta_1 = r_1[(r_M/r_1)^{1/2(M-1)} - 1] \qquad j = 1 \tag{III-8}$$

$$\Delta_j = r_1(r_M/r_1)^{(j-3/2)/(M-1)}[(r_M/r_1)^{1/(M-1)} - 1] \qquad j \neq 1, j \neq M \tag{III-9}$$

$$\Delta_M = r_M - r_1(r_M/r_1)^{(M-3/2)/(M-1)} \qquad j = M \tag{III-10}$$

$$k_j = g\rho r_j^2/3\eta\bar{z} \tag{III-11}$$

$$q_j = \frac{1}{\Delta_j}\left|\frac{\mathrm{d}r}{\mathrm{d}t}\right| = \frac{1}{\Delta_j}\left|\frac{3RTk_{\text{tr}}r_j(C_{\text{bulk}} - C^0_{\text{sat}} - 2\kappa\sigma/r_j)}{3P_{\text{atm}}r_j + 4\sigma}\right| \tag{III-12}$$

Equation III-1 defines the quantity measured experimentally.

Equations III-2 and III-3 assume Henry's law is applicable.

Equation III-4 is a well-known equation of surface chemistry. A derivation is summarized in ref 4.

Equation III-5 follows from manipulation of eq III-2 and III-4. It neglects hydrostatic pressure due to solution itself when a bubble is below the surface.

Equation III-6 involves a slight approximation because it uses C^0_{sat} instead of the more rigorous C_{sat} as in eq III-5. If this approximation were not invoked, the r's and Δ's would become variables influenced by the value of ΔP, and the computations would become much more complicated.

Equation III-7 makes log r_j a linear function of j. The implications are discussed in section VII-2.

Equations III-8 to III-10 assign the boundary, r_b, between radius increments r_j and r_{j+1} in such a way that log r_b = (log r_j + log r_{j+1})/2.

Equation III-11 is based on hydrostatic assumptions discussed in ref 6.

Equation III-12 invokes eq 7 in ref 4. It involves the same approximation as that in eq III-6 and would be more rigorous if C^0_{sat} and P_{atm} were replaced by C_{sat} and P_{gas}, respectively. Such substitutions would complicate the computations to little purpose.

IV. Dynamic Equations

The variables describing the state of the system as a whole are C_{bulk}, ΔP, and $N_1, ..., N_j, ..., N_M$. The dynamic equations describing these variables as functions of time are IV-1 to IV-15:

$$\frac{\mathrm{d}C_{\text{bulk}}}{\mathrm{d}t} = \Phi_{\text{reac}} - k_{\text{ex}}\frac{A}{V_s}(C_{\text{bulk}} - C_{\text{sat}}) - \frac{4\pi r_1^3}{3RT}P_1 J - \sum_{j=1}^{M} 4\pi r_j^2 k_{\text{tr}} N_j (C_{\text{bulk}} - \kappa P_j) \tag{IV-1}$$

$$v_{\text{esc}} = k_{\text{ex}}A(C_{\text{bulk}} - C_{\text{sat}}) + \sum_{j=1}^{M}\frac{4\pi r_j^3 P_j k_j V_s N_j}{3RT} \tag{IV-2}$$

$$\mathrm{d}\Delta P/\mathrm{d}t = v_{\text{esc}}F - k_{\text{cap}}\Delta P \tag{IV-3}$$

$$F = 760\ \frac{\text{torr}}{\text{atm}}\ 82.053\ \frac{\text{cm}^3\ \text{atm}}{\text{mol K}}\ \frac{T}{V_g}\ \frac{\text{K}}{\text{cm}^3} \tag{IV-4}$$

$$\Delta P_{\text{ss}} = \Phi_{\text{reac}}V_s F/k_{\text{cap}} \tag{IV-5}$$

$$k_{\text{ex}}(\text{crit}) = \Phi_{\text{reac}}V_s/A(C_{\text{crit}} - C_{\text{sat}}) \tag{IV-6}$$

$$\Phi_{\text{crit}} = k_{\text{ex}}A(C_{\text{crit}} - C_{\text{sat}})/V_s \tag{IV-7}$$

$$\Phi_{\text{xs}} = \Phi_{\text{reac}} - \Phi_{\text{crit}} \tag{IV-8}$$

$$J = \alpha \exp[-\beta/(C - C_{\text{crit}})^2] \tag{IV-9}$$

If $r_j > r_{\text{eq}}$

$$\mathrm{d}N_1/\mathrm{d}t = J - (q_1 + k_1)N_1 \qquad j = 1 \tag{IV-10}$$

$$\mathrm{d}N_j/\mathrm{d}t = q_{j-1}N_{j-1} - (q_j + k_j)N_j \qquad j \neq 1, j \neq \mathrm{M} \tag{IV-11}$$

$$\mathrm{d}N_M/\mathrm{d}t = q_{M-1}N_{M-1} - k_M N_M \qquad j = M \tag{IV-12}$$

If $r_j < r_{\text{eq}}$

$$\mathrm{d}N_j/\mathrm{d}t = q_{j+1}N_{j+1} - (q_j + k_j)N_j \qquad j \neq M \tag{IV-13}$$

$$\mathrm{d}N_M/\mathrm{d}t = -(q_M + k_M)N_M \qquad j = M \tag{IV-14}$$

If $r_j = r_{\text{eq}}$

$$\mathrm{d}N_j/\mathrm{d}t = -k_j N_j \qquad j = 1, ..., M \tag{IV-15}$$

Equation IV-1 is equivalent to eq 32 in ref 5. The first negative term describes evaporation of molecules from the surface of the stirred solution. The second negative term describes loss of molecules by formation of nuclei and is probably negligible. The summation describes interchange of molecules between bulk solution and bubbles of various sizes; individual terms may be positive or negative.

Equation IV-2 is the total rate of transfer of CO from solution to gas either by evaporation of molecules or by escape of bubbles of various sizes. The terms in the summation are all positive.

Equation IV-3 describes the change of pressure in the flask due to transfer of gas from solution and escape through the capillary leak.

Equation IV-4 defines the conversion factor F used to relate moles of product gas to pressure generated in the flask.

Equation IV-5 is derived from eq IV-3 for the steady state in which $\mathrm{d}\Delta P/\mathrm{d}t = 0$ and $v_{\text{esc}} = \Phi_{\text{reac}}V_s$.

Equations IV-6 and IV-7 are each derived from eq IV-1 for the steady state in which there are no bubbles and $C_{\text{bulk}} = C_{\text{crit}}$.

Equation IV-8 defines a quantity of importance to the subsequent development.

Equation IV-9 describes the rate of nucleation and is discussed in ref 6.

Equations IV-10 to IV-12 describe rates of change of increment for those bubbles large enough to grow in that solution.

Equations IV-13 and IV-14 describe rates of change of increment for those bubbles so small that they tend to shrink.

Equation IV-15 describes physical escape of those bubbles having no net tendency either to grow or to shrink.

TABLE I: Experimentally Determined Periods and Amplitudes

system designation	time since mixing/min	$10^6\Phi_{reac}$/mol cm^{-3} s^{-1}	τ/s	$\Delta P_{max}/\Delta P_{min}$	$\Delta P_{max}/\Delta P_{ss}$	$10^3 k_{ex}$(crit)/cm s^{-1}
I	5	3.10	~16	~6.3	~2.1	42.1
II	10	2.24	13–19	7.5–8.2	2.2–2.7	30.4
III	15	1.64	15–20	6.3–6.4	2.2–2.6	22.3
IV	20	1.34	16–20	3.8–5.3	1.9–2.3	18.2
V	25	1.07	~15	~3.3	~1.8	14.5
VI	30	0.88	~13	~2.3	~1.5	12.0

V. Numerical Values of Parameters

The following parameter values were used for the computations described in section VI:

$$A = 29.8 \text{ cm}^2$$

$$C_{crit} = 7.0 \times 10^{-5} \text{ mol cm}^{-3}$$

$$C^0_{sat} = 8.2 \times 10^{-7} \text{ mol cm}^{-3}$$

$$g = 980 \text{ cm s}^{-2}$$

$$k_{cap} = 0.579 \text{ s}^{-1}$$

$$k_j = 6.82 \times 10^3 (r_j/\text{cm})^2 \text{ s}^{-1}$$

$$M = 60$$

$$P_{atm} = 760 \text{ torr}$$

$$r_1 = 1.2803 \times 10^{-6} \text{ cm}$$

$$r_M = 0.1 \text{ cm}$$

$$R = 6.236 \times 10^4 \text{ cm}^3 \text{ torr mol}^{-1} \text{ K}^{-1}$$

$$T = 40 \text{ °C} = 313.15 \text{ K}$$

$$V_g = 178 \text{ cm}^3$$

$$V_s = 28 \text{ cm}^3$$

$$\bar{z} = 0.595 \text{ cm}$$

$$\alpha = 1 \times 10^{48} \text{ cm}^{-3} \text{ s}^{-1}$$

$$\beta = 5 \times 10^{-7} \text{ mol}^2 \text{ cm}^{-6}$$

$$\eta = 0.145 \text{ g cm}^{-1} \text{ s}^{-1}$$

$$\kappa = 1.08 \times 10^{-9} \text{ mol cm}^{-3} \text{ torr}^{-1}$$

$$\rho = 1.8 \text{ g cm}^{-3}$$

$$\sigma = 55 \text{ dyn cm}^{-1} = 0.041 \text{ torr cm}$$

Reasons for selecting most of these values follow directly from material in ref 6 and 7.

The value of r_1 was obtained from eq III-6. The number of significant figures is probably unnecessarily large, but this value was selected after some preliminary computations with 1×10^{-6} and 2×10^{-6} cm occasionally gave absurd results when Φ_{reac} was close to Φ_{crit}.

Reasons for selection of values for M and r_M are discussed in section VII-2.

The program reduced problems with underflows by setting $J = 0$ whenever $\log J < -35$.

Computations used six values of Φ ranging between $10^6\Phi = 3.10$ and 0.88 mol cm^{-3} s^{-1}. The bases for these values are discussed in section VI.

The value of k_{ex} was treated as a disposable parameter and varied from 0.004 to 0.04 cm s^{-1}. These numbers seem excessive when compared to the value of k_{tr} derived from material in ref 7. The implications are discussed in section VII-4.

VI. Results

TABLE II: Computed Periods and Amplitudes[a]

system designation	$10^3 k_{ex}$/ cm s^{-1}	τ/s	$\Delta P_{max}/\Delta P_{min}$	$\Delta P_{max}/\Delta P_{ss}$
I	8	32.6	64	7.2
	10	32.2	54	7.4
	12	31.8	47	7.4
	16	30.8	33	7.2
	20	28.4	20	6.3
	25	23.2	9.0	4.5
	*†30	16.6	3.7	2.6
	35	10.6	1.69	1.44
	40	7.9	1.10	1.07
II	8	32.9	54	8.7
	10	30.7	35	7.8
	12	27.9	22	6.8
	16	21.7	9.4	4.5
	*†18	18.4	6.1	3.4
	20	15.4	4.0	2.6
	25	9.4	1.58	1.36
III	8	23.1	18	5.8
	10	19.5	10	4.4
	*†12	15.9	5.9	3.2
	16	10.5	2.2	1.69
	20	8.0	1.22	1.15
IV	6	20.0	16	5.1
	*7	18.0	12	4.4
	8	16.2	8.3	3.7
	†10	13.1	4.5	2.6
	12	10.5	2.6	1.84
	16	8.0	1.27	1.18
V	*5	15.4	11	3.9
	6	13.8	7.5	3.2
	7	12.3	5.2	2.7
	†8	11.0	3.7	2.2
	10	9.0	2.0	1.58
VI	*4	13.1	9.1	3.3
	5	11.6	5.8	2.7
	6	10.5	3.8	2.2
	7	9.6	2.7	1.83
	†8	8.8	2.0	1.56
	10	8.2	1.39	1.24

[a] An * denotes the computation selected as best to represent period, and a † the computation selected as best to represent amplitude.

Computations were carried out for six different values of $10^6\Phi_{reac}$ ranging from 3.10 to 0.88 mol cm^{-3} s^{-1}. Those values were chosen to represent rates of reaction under the conditions of ref 7 for solutions at 5-min intervals 5 to 30 min after mixing. These solutions were assigned the designations I to VI and are identified in Table I along with experimentally observed periods and amplitudes for two ostensibly identical runs as described in ref 7. The last column in this table presents the critical k_{ex} values above which gas would escape smoothly from solution without nucleating any bubbles.

For each of these six solutions, we made computations for several values of $10^3 k_{ex}$ all of which fell between 4 and 40 cm s^{-1}. The simultaneous equations were integrated by the Gear[8] algorithm with use of the PDP 1091 computer at the University of Oregon. Each of the 38 computations reported in Table II used $M = 60$ and $r_M = 0.1$ cm. The initial value of C_{bulk} was selected to be less than C_{crit} but large enough that C_{crit} was attained in a time which was not too long. The exact selection of initial concentration was immaterial because the system seemed to follow

---

[8] Hindmarsh, A. C. "Gear. Ordinary Differential Equation Solver", UCID-30001 Rev 3; Lawrence Livermore Laboratory: Livermore, CA, 1974.

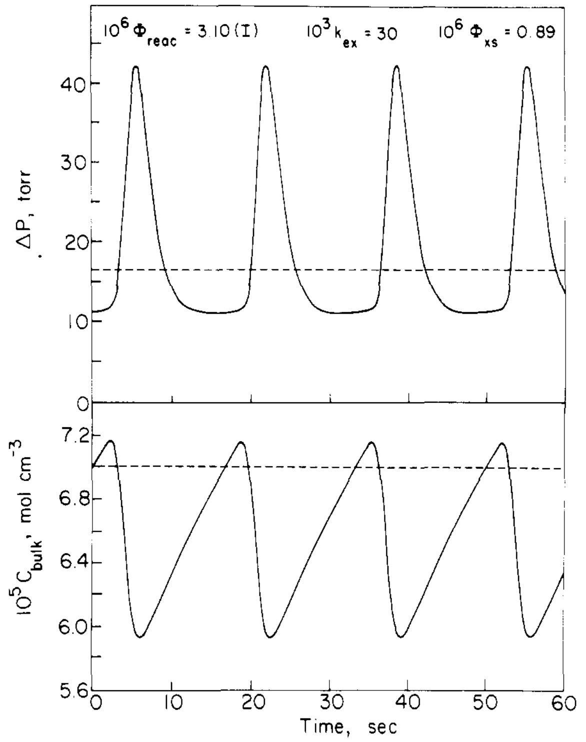

Figure 1. Computations modeling concentration and pressure best reproducing the experimental period for system I.

limit cycle behavior at all times after the first maximum in ΔP. Characteristics of the computed periodic behaviors are summarized in Table II.

The computations in Table II generate ranges of periods and amplitudes which exceed the rather ill-defined ranges suggested by the two experimental runs described in ref 7. For each of the six designated systems, an * is used to indicate the computation we rather arbitrarily select as best reproducing the experimental period, while a † is used to indicate the best representation of the experimental amplitude. The experimental values are sufficiently uncertain that it is often impossible to justify a strong preference between adjacent lines in Table II. Within those uncertainties, the same k_{ex} could reproduce both period and amplitude satisfactorily for the three systems with the largest rates of chemical reaction. For the three systems where reaction was slower, the k_{ex} which best reproduced the period was smaller than that which best reproduced the amplitude. For all systems, experimental values of $\Delta P_{max}/\Delta P_{min}$ were reproduced by slightly smaller values of k_{ex} than were experimental values of $\Delta P_{max}/\Delta P_{ss}$. The reasons for this effect are discussed in section VII-1.

Examination of the results of these computations indicates that behavior in different runs can be described remarkably well in terms of the value of the single parameter Φ_{xs}, the excess of the rate of production of dissolved gas over the rate at which gas molecules would evaporate from the surface of the solution in a steady state such that $C_{bulk} = C_{crit}$. Table III orders the 38 computational runs of Table II according to decreasing values of Φ_{xs}. The period, τ, is slightly dependent upon Φ_{reac} for runs with the same value of Φ_{xs}, but the effect is scarcely detectable. The maximum and minimum values of concentration are even more nearly monotonic functions of Φ_{xs} without regard for any other parameter values.

The last five columns in Table III give the times within a period at which extreme and critical values of concentration and of pressure were attained. Time zero was always defined to be when increasing concentration attained $C_{crit} = 7.000 \times 10^{-5}$ mol cm^{-3}. The computations reported values of variables every 0.2 s, and these values were mentally interpolated to estimate important times to 0.1 s. Periods and times in the last six columns of Table III could therefore be in error by up to 0.2 s. Internal consistency of the entries suggests that average errors are considerably less than this.

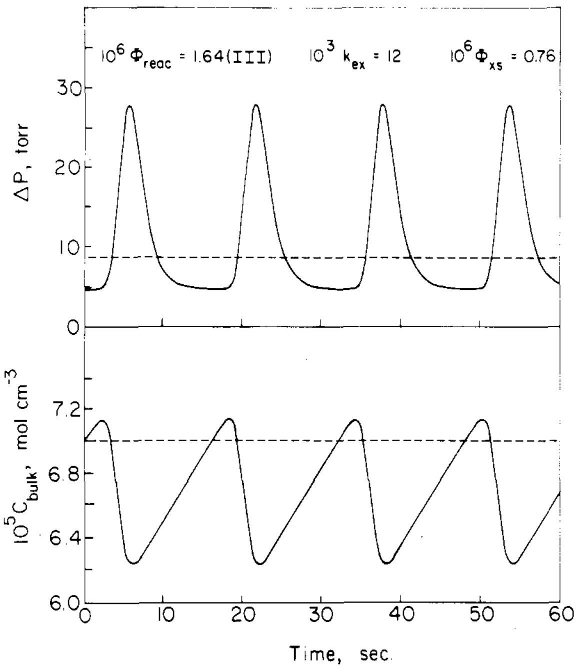

Figure 2. Computations best reproducing the experimental period for system III.

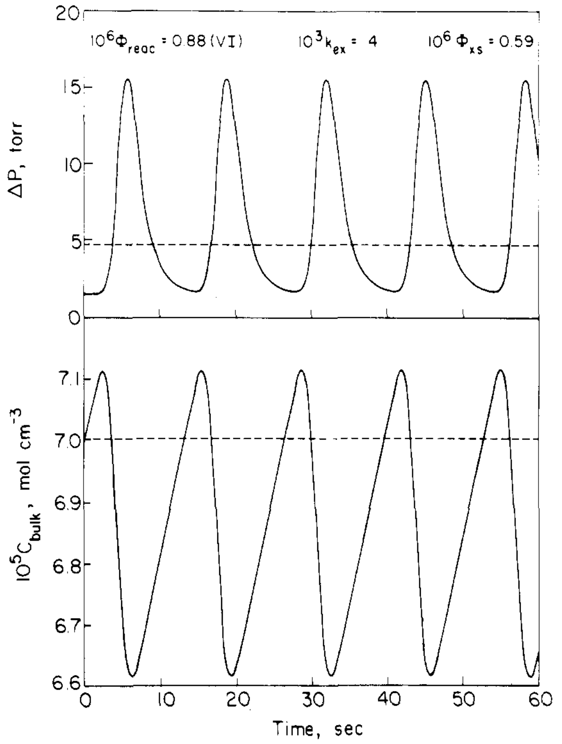

Figure 3. Computations best reproducing the experimental period for system VI. Note that the amplitude of C_{bulk} oscillations is reduced from those in Figures 1 and 2.

The results of 5 of these 38 computations are shown in the figures. Each figure assigns time zero when C_{bulk} first attained C_{crit}, and each continues for 60 s. The dashed horizontal line in each C_{bulk} plot corresponds to C_{crit}. The ordinates of all ΔP plots start at zero, and each dashed horizontal line is the value of ΔP_{ss} which would occur if gas were evolved smoothly instead of in pulses. Therefore, ΔP plots in these figures can be compared with the experimental runs in ref 7.

Figures 1–3 show plots for the values of k_{ex} selected in Table II to best reproduce the experimental period for systems I, III, and VI. Figures 4 and 5 show plots for extreme values of Φ_{xs} for two computations of system I with $\Phi_{reac} = 3.1 \times 10^{-6}$ mol cm^{-3} s^{-1}. These two figures can be compared with the intermediate

TABLE III: Oscillatory Solution Behavior as a Function of Φ_{xs}[a]

$10^6\Phi_{xs}$/ mol cm^{-3} s^{-1}	$10^6\Phi_{reac}$/ mol cm^{-3} s^{-1}	10^3k_{ex}/ cm s^{-1}	10^5C_{max}/ mol cm^{-3}	10^5C_{min}/ mol cm^{-3}	τ/s	times during period, s C_{max}	C_{crit}	C_{min}	P_{max}	P_{min}
2.51	3.10 (I)	8	7.299	0.513	32.6	1.4	1.7	5.2	4.4	21.9
2.36	3.10 (I)	10	7.293	0.638	32.2	1.4	1.8	5.4	4.4	20.4
2.22	3.10 (I)	12	7.278	0.824	31.8	1.5	1.8	5.5	4.5	19.0
1.92	3.10 (I)	16	7.258	1.450	30.8	1.6	2.0	5.7	4.7	16.9
1.65	2.24 (II)	8	7.237	2.231	32.9	1.7	2.2	6.1	4.8	17.8
1.63	3.10 (I)	20	7.232	2.543	28.4	1.7	2.3	5.9	4.9	15.9
1.50	2.24 (II)	10	7.223	2.930	30.7	1.7	2.3	6.0	4.9	17.1
1.36	2.24 (II)	12	7.210	3.684	27.9	1.7	2.4	6.0	5.0	16.6
1.26	3.10 (I)	25	7.197	4.352	23.2	1.9	2.5	5.8	5.1	15.1
1.06	2.24 (II)	16	7.178	5.166	21.7	2.0	2.8	5.9	5.2	15.8
1.05	1.64 (III)	8	7.176	5.133	23.1	2.0	2.8	6.0	5.3	17.1
0.91	2.24 (II)*†	18	7.159	5.773	18.4	2.1	3.0	5.9	5.3	15.3
0.90	1.64 (III)	10	7.158	5.757	19.5	2.2	3.0	6.1	5.4	16.5
0.90	1.34 (IV)	6	7.158	5.748	20.0	2.2	3.0	6.1	5.4	17.5
0.89	3.10 (I)*†	30	7.154	5.931	16.6	2.1	3.1	5.9	5.4	14.4
0.82	1.34 (IV)*	7	7.148	6.014	18.0	2.2	3.2	6.1	5.5	17.1
0.77	2.24 (II)	20	7.138	6.252	15.4	2.2	3.3	6.0	5.5	15.1
0.76	1.64 (III)*†	12	7.138	6.247	15.9	2.3	3.3	6.0	5.5	16.0
0.75	1.34 (IV)	8	7.137	6.244	16.2	2.2	3.3	6.0	5.6	16.7
0.71	1.07 (V)*	5	7.131	6.363	15.4	2.3	3.3	6.0	5.5	16.6
0.63	1.07 (V)	6	7.118	6.537	13.8	2.3	3.5	6.1	5.6	15.2
0.60	1.34 (IV)†	10	7.114	6.597	13.1	2.4	3.6	6.0	5.7	14.6
0.59	0.88 (VI)*	4	7.112	6.616	13.1	2.4	3.6	6.1	5.7	14.7
0.55	1.07 (V)	7	7.106	6.677	12.3	2.4	3.7	6.1	5.7	13.8
0.52	3.10 (I)	35	7.097	6.770	10.6	2.4	3.8	6.0	5.7	12.4
0.52	0.88 (VI)	5	7.099	6.740	11.6	2.4	3.7	6.1	5.7	13.4
0.48	1.07 (V)†	8	7.093	6.786	11.0	2.4	3.8	6.0	5.8	12.9
0.46	1.64 (III)	16	7.089	6.818	10.5	2.4	3.9	6.1	5.8	12.4
0.46	1.34 (IV)	12	7.088	6.820	10.5	2.5	4.0	6.2	5.9	12.5
0.44	0.88 (VI)	6	7.085	6.834	10.5	2.5	4.0	6.1	5.8	12.4
0.40	2.24 (II)	25	7.076	6.886	9.4	2.5	4.1	6.1	5.9	11.6
0.36	0.88 (VI)	7	7.071	6.900	9.6	2.4	4.1	6.1	5.9	11.5
0.33	1.07 (V)	10	7.065	6.922	9.0	2.6	4.3	6.2	5.9	11.3
0.29	0.88 (VI)†	8	7.056	6.944	8.8	2.4	4.2	6.1	5.8	10.8
0.17	1.64 (III)	20	7.030	6.975	8.0	2.3	4.2	5.9	5.7	10.2
0.16	3.10 (I)	40	7.027	6.978	7.9	2.3	4.1	5.8	5.7	10.1
0.16	1.34 (IV)	16	7.029	6.975	8.0	2.3	4.1	5.9	5.7	10.2
0.14	0.88 (VI)	10	7.026	6.976	8.2	2.3	4.0	5.7	5.6	10.3

[a] An * denotes the computation selected as best to represent experimental period and a † the computation selected as best to represent experimental amplitude.

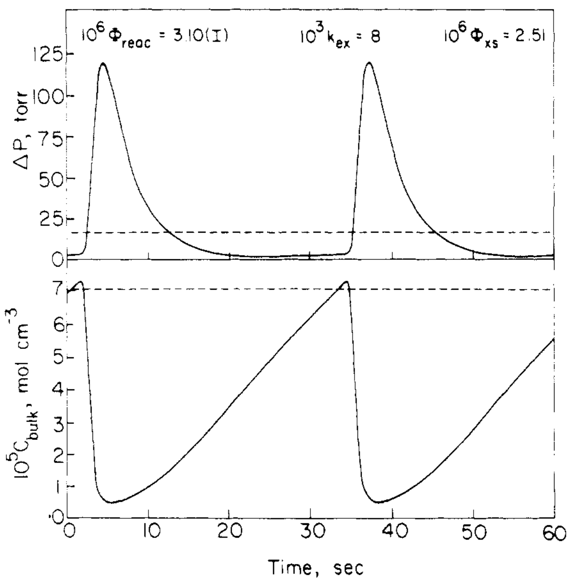

Figure 4. Computations for a representative of system I having the maximum value of Φ_{xs} examined. Note that the ordinate of the C_{bulk} plot goes to zero and that ΔP_{max} is about 7 times ΔP_{ss}.

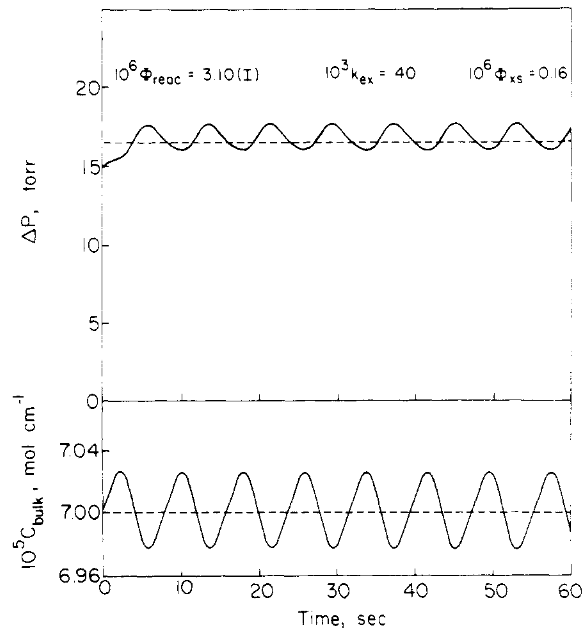

Figure 5. Computations of a representative of system I having the minimum value of Φ_{xs} examined. Note that the approximately sinusoidal oscillations in C_{bulk} have an amplitude only about 1% of the average concentration and that the amplitude of the ΔP oscillations would also be too small for easy experimental observation.

situation of Figure 1 for the same value of Φ_{reac}.

VII. Discussion

1. Qualitative Comparison of Computation and Experiment. It is instructive to compare the plots in Figures 1–3 with the experimental traces in Figure 3 of ref 7. The computations reproduce the experimental feature that the pressure rises more rapidly than it falls after the maximum. The computations in ref 4 generated a slower rise and more rapid fall in pressure. It is encouraging that our putative improvements in the model also generate a greater consistency with reality.

Neither the experimental nor the computed curves resemble true sine functions. The value of ΔP rises above ΔP_{ss} for less than half a period but goes more above ΔP_{ss} during this time than it falls below during the larger portion of the period. The computed pressures spend a somewhat greater fraction of a period below the steady-state value than do the experimental values, but the difference is not large.

The asymmetry of a periodic function can be designated μ defined by

$$\mu = \frac{\Delta P_{\max} - \Delta P_{ss}}{\Delta P_{ss} - \Delta P_{\min}} \tag{VII-1}$$

For the experimental curves summarized in Table IV of ref 7, μ is about 1.7 to 2.7 for the first 20 min and falls to 1.35 at 30 min after preparation of the solution. For the computations marked with an * in Table II, μ is 4.7 to 5.6 for the first 20 min and falls to 4.3 at 30 min. We believe that at least part of the discrepancy arises from an artifactual error in the computations as discussed in subsection 3. Possible corrections in the model are discussed in subsection 8.

2. Selection of M and of r_M. The computational procedure cannot integrate continuous functions but must consider populations centered on incrementally different radii. Of course the larger the value of M the greater the accuracy and the greater the cost of the computations. The selection of $M = 60$ was a compromise influenced by a consistency test discussed in subsection 3.

The maximum radius was selected to be 0.1 cm. For this size of bubble, eq III-11 leads to $k_M = 68\ \mathrm{s}^{-1}$, and an average bubble would only persist 15 ms in solution before it escaped. For $M = 60$, substitution into eq III-12 leads to $q_M = 0.68\ \mathrm{s}^{-1}$. Therefore, a bubble of 0.1-cm radius has 100 times as much likelihood to escape the solution as to grow to the next increment of size, and the time for escape is very short compared to the period of the oscillations being modeled. It would be pointless to include consideration of any larger bubbles.

3. Consistency Tests for Computational Accuracy. If the equations are intergrated over an integral number of periods, the argument requires that the average value of v_{esc} must equal $\Phi_{reac}V_s$. The program satisfied this constraint precisely whenever k_{ex} was so large that the steady-state concentration was less than C_{crit}. In such situations, all gas was escaping from the surface of the solution without forming significant numbers of bubbles.

If k_{ex} was reduced enough that the program was modeling oscillatory release of bubbles, the average value of v_{esc} was greater than $\Phi_{reac}V_s$. For some computations with $10^6\Phi_{reac} = 1.3\ \mathrm{mol\ cm^{-3}\ s^{-1}}$ and $10^3 k_{ex} = 8\ \mathrm{cm\ s^{-1}}$, the discrepancies were 32.5%, 21.3%, and 16.3% for M values of 40, 60, and 80, respectively. These errors are inversely proportional to M and could apparently be eliminated entirely by the impractical expedient of using an indefinitely large number of radius increments. For these three computations, the values of μ defined by eq VII-1 were 5.15, 4.43, and 4.12, respectively. These values suggest that as M increased indefinitely μ might approach but not attain the experimental value of up to 2.2. It is worth noting that computations with all three values of M gave the same period of 15 s.

These discrepancies indicate that when bubbles are produced the program transfers more moles of CO from solution to gas than are being produced by chemical reaction. We could not find any mistake of logic in the program, and the inverse dependence of error size on M strongly suggests that the problem arises from the finite widths of successive radius increments. The rate constant k_j for escape of a bubble is proportional to r_j^2, and the number of moles of gas in a bubble is proportional to r_j^3. Therefore, the effective rate constant for transfer of material from solution to gas varies approximately as j^5! Even with $M = 60$, successive increments of radius increase by factors of 20.7%, and rate constants for gas escape increase by factors of 2.56. The program in its present form is too coarse-grained for precise pressure computations.

The argument also requires that over an integral number of periods the average value of the summation in eq IV-2 must equal[9] V_s times the value of the summation in eq IV-1. When we attempted to test this further constraint, we found that the summation in eq IV-2 was greater than V_s times that in eq IV-1 by almost precisely the amount by which v_{esc} exceeded $\Phi_{reac}V_s$. For evaporation into bubbles of different incremental radii, the rate constants in eq IV-1 vary approximately as j^2 instead of the j^5 in eq IV-2. We believe the program is sufficiently fine-grained that it reproduces well the temporal variation of C_{bulk} even though it fails to be exact for the variation of ΔP.

4. Significance of Chosen k_{ex} Values. When this project was undertaken, it was hoped that experimental behavior could be reproduced by employing parameters *all* of which had been measured independently. That expectation was unduly optimistic for reasons which are now apparent.

As described in ref 7, the rate constant k_{ex} was measured at different stirring rates for solutions of sulfuric acid alone. When formic acid was also present, oscillatory gas evolution was observed at stirring rates such that $10^3 k_{ex}$ would have been 1.1 to 1.7 cm s^{-1} for sulfuric acid alone. Substitution of those values into the computations failed miserably to reproduce the experimental observations. However, Table II shows that experimental behavior could be modeled very satisfactorily with selected $10^3 k_{ex}$ values between 4 and 30 cm s^{-1}.

The reason for the discrepancy is obvious in retrospect. The measurements with sulfuric acid alone took place with evaporation of gas molecules through a surface having a constant area of 29.8 cm^2. When pulsed evolution of gas takes place, each pulse is accompanied by formation of a considerable amount of *foam*. The bubbles in that foam escape more slowly than calculated by simple hydrodynamics, and the surface area available to evaporation of gas is much greater than it would be in the absence of foam.

The program treats $k_{ex}A$ as a constant in eq IV-1 and IV-2. We kept $A = 29.8\ \mathrm{cm}^2$ and treated k_{ex} as a constant disposable parameter which was larger for those situations in which more foam would be anticipated. Alternative modeling procedures are discussed in subsection 8.

5. Ranges of Computed Concentrations. The first semiquantitative efforts to model this system[4] assumed k_j was independent of r_j. Those computations failed to reproduce some qualitative features of the observed ΔP traces as mentioned in subsection 1.

Those previous computations[4] also indicated that C_{bulk} fell to about 20% of C_{crit} before it began to rise again. For the computations designated with an * in Table III, C_{bulk} always lies in the much narrower range of 80% to 102% of C_{crit}. If a technology could be developed to measure the concentration of dissolved gas as a continuous function of time, experimental tests of our model might be more demanding than the present ones based on pressure measurements. Tests based on concentration would be particularly desirable because the discussion in subsection 4 suggests that ΔP values based on eq IV-2 and IV-3 are impacted by computational artifacts which are much less severe for C_{bulk} values based on eq IV-1.

6. Variation of Behavior with Φ_{xs}. As was pointed out in section VI, it is remarkable how well computations at different values of Φ_{reac} can be ordered in terms of the single parameter Φ_{xs}, the excess of reaction rate over that necessary to attain a steady-state concentration equal to C_{crit}.

The entries in Table III fall into two types of behavior roughly identified by whether Φ_{xs} is greater or less than 1.0×10^{-6} mol $\mathrm{cm^{-3}\ s^{-1}}$. If Φ_{xs} is less than this value, the concentration is always at least 80% of C_{crit} and the period is 8 to 20 s. For larger values of Φ_{xs}, the minimum concentration is much reduced, and for the run in Figure 4 it is only 7% of C_{crit}. The periods in these runs are lengthened to as much as 33 s.

---

[9] This assertion of exact equality neglects the trivial $4\pi J r_1^3 P_1/3RT$ term in eq IV-1.

For the runs with $10^6\Phi_{xs} < 1$ mol cm^{-3} s^{-1}, the concentration reaches its maximum value 2 to 2.5 s after it has reached C_{crit} and will return to C_{crit} after a total time of 3 to 4 s after that value was first attained. The larger the value of Φ_{xs}, the larger the maximum concentration which is attained, but the time during which nucleation can occur is constant to within about 1 s. For these same runs, the concentration falls to its minimum value almost precisely 6 s after nucleation was initiated. The pressure in the flask reaches its maximum up to 0.7 s before the concentration minimum. The time of minimum pressure is almost always within about 2 s of the time that nucleation begins for the next pulse.

The computations with $10^6\Phi_{xs} > 1$ mol cm^{-3} s^{-1} describe systems which probably could not be prepared experimentally. For these computations, the concentration maximum is less symmetrical, and there is a more precipitous fall. No matter how far the concentration drops, the minimum is always attained 5.2 to 6 s after nucleation first began, and the pressure reaches its rather high maximum up to 1 s before the concentration minimum. In these runs, the pressure reaches its minimum not much longer after nucleation than it does in the other runs, but the time until the start of the next period is up to 15 s longer because the depleted concentration must first be restored.

For all of the runs in Table III, and particularly for the ones of potential experimental interest where $10^6\Phi_{xs} < 1$ mol cm^{-3} s^{-1}, there is surprisingly little variation of the times after nucleation at which different events occur. We have not tried to fit those times to the elegant analytical expressions recently developed by Engelking[10] to describe times for growth and escape of bubbles. However, the evidence that such times are little impacted by rates of stirring or of chemical reaction reinforces the hope expressed in ref 4 that differential difference equations might permit a rather simple semiquantitative modeling of this system. We lack the mathematical sophistication to undertake such modeling ourselves.

7. Large and Small Limiting Reaction Rates. Experimental observations[3,7,11] indicate that oscillations do not occur near the start of a run when the rate of gas production is larger nor near the end when the rate is slow. Increased stirring rate can also suppress oscillations, particularly near the end of a run.

The computations reported here are consistent with the experimental observations near the end of a run. As Φ_{reac} is reduced or as k_{ex} is increased (to suggest increased stirring rate), the computed amplitude of the oscillations decreases while they become more sinusoidal and of somewhat shorter period. The computed oscillations would disappear when k_{ex} had been reduced to k_{ex}(crit) calculated for the Φ_{reac} used in the computations. In an experimental system, the oscillations would disappear into the random noise even before Φ_{reac} had fallen to the Φ_{crit} for the stirring employed.

The failure to oscillate at large reaction rates cannot be handled by the present model, which assumes a uniform system. If mixing is not sufficiently rapid, the concentration will attain C_{crit} at different times in different regions, and a chaotic evolution of gas bubbles would wipe out any periodicities. Such a situation is obviously beyond the capabilities of this model.

8. Possible Improvements in the Model. The above discussion has revealed two specific ways in which the model could be improved. In subsections 2 and 3, it was shown that even 60 increments of radius was too coarse-grained to handle the strong dependence on size of the rate constant for removal of gas in large bubbles. In subsection 4, it was pointed out that the $k_{ex}A$ measured for escape of gas from stirred sulfuric acid was not really appropriate to use in eq IV-1 and IV-2 to model evaporation from a liquid which underwent foaming during various portions of a cycle.

The problem due to radius increments could be reduced by noting that the logarithmic scaling we used in eq III-7 is very appropriate for small bubbles but not for large ones. The equations developed here might be used for $r_j \leqslant 0.01$ cm, and the radius increments from this value to $r_M = 0.1$ cm might be constant at $\Delta_j = 0.003$ cm. It might well turn out that effective modeling might be obtained with $r_M = 0.05$ cm, thereby considerably reducing the necessary number of radius increments of constant size.

The substitution for $k_{ex}A$ would be more complicated because this quantity should vary during a cycle. An appropriate procedure might be to replace it in eq IV-1 and IV-2 with $k'_{ex}A + GS$. Here k'_{ex} would be the experimentally measured k_{ex} of 0.011 to 0.017 cm s^{-1}, A would be the experimental 29.8 cm^2, S would be the summation in eq IV-2, and G would be a disposable parameter. The rationale for this approach is to note that S is proportional to the rate at which gas is escaping the solution in bubbles and is therefore an approximation to the rate of foaming. The critical test of this approach would be whether a single value of G could model all six of the situations in Table I to within the moderately large range of experimental uncertainty.

The program as developed here assumes bulk composition is everywhere the same and fails to note the variations arising because growth and rise of large bubbles are monotonic functions. Therefore, bubbles in the upper part of the solution will tend to be larger than those further down. This tendency will be impacted by stirring in ill-defined ways.

Modeling refinements and increasing numbers of parameters can always be made to improve the accuracy of a set of computations. We doubt that the suggestions made here would be worth the effort. We believe we can fairly say that the problem is now understood and that seldom, if ever, has a system as complicated as this one been modeled with such good fidelity.

Acknowledgment. Peter Ruoff received a grant from the Norwegian Research Council for Science and Technology (NTNF). This work was supported in part by a grant from the National Science Foundation. Dr. S. M. Kaushik made some of the preliminary computations while procedures were being developed.

Registry No. HCOOH, 64-18-6; H_2SO_4, 7664-93-9; CO, 630-08-0.

---

[10] Engelking, P. C. *J. Phys. Chem.* **1985**, *89*, 1520–1523.

[11] Showalter, K.; Noyes, R. M. *J. Am. Chem. Soc.* **1978**, *100*, 1042–1049.